Supporting information

New Pd(II)-pincer type complexes as potential antitumor drugs: Synthesis, nucleophilic substitution reactions, DNA/HSA interaction, molecular docking study and cytotoxic activity

Sladjana Pavlović,[a] Biljana Petrović,[b] Dušan Ćoćić,[b] Andreas Schreurer,[c] Snežana Sretenović,[d] Maja D. Nešić,[e] Marija Nišavić,[e] Zorana Maric,[f] Isidora Stanisavljević,[a] Irfan Ćorović,[g] Bojana Simović Marković,[a] Veljko Maric,[f] Ivan Jovanović,[a] Gordana Radić,[h] Snežana Radisavljević,*[b] and Snežana Jovanović Stević,*[h]

[a]*University of Kragujevac, Faculty of Medical Sciences, Center for molecular medicine and stem cell research, Svetozara Markovića 69, 34000 Kragujevac, Serbia*

[b]*University of Kragujevac, Faculty of Science, Department of Chemistry, Radoja Domanovića 12, 34000 Kragujevac, Serbia*

[c]*Inorganic Chemistry, Department of Chemistry and Pharmacy, University of Erlangen-Nürnberg, Erlangen, Germany*

[d]*University of Kragujevac, Faculty of Medicinal Science, Department of Internal Medicine, Kragujevac, Serbia*

[e]*Center for Light-Based Research and Technologies COHERENCE, Department of Atomic Physics, Vinča Institute of Nuclear Sciences, National Institute of the Republic of Serbia, University of Belgrade, 11000*

[f]*University of East Sarajevo, Faculty of medicine, Studentska 5, 73300 Foca, BiH*

[g]*General Hospital of Novi Pazar, Department of Internal Medicine, Generala Živkovića 1, 36300 Novi Pazar, Serbia*

[h]*University of Kragujevac, Faculty of Medical Sciences, Department of Pharmacy, Svetozara Markovića 69, 34000 Kragujevac, Serbia*

Corresponding authors:

Snežana Jovanović Stević, Phone: +381(0)34306800, Email: snezanaj@kg.ac.rs;

Snežana Radisavljević, Phone: +381(0)34336223, Email: snezana.radisavljevic@pmf.kg.ac.rs

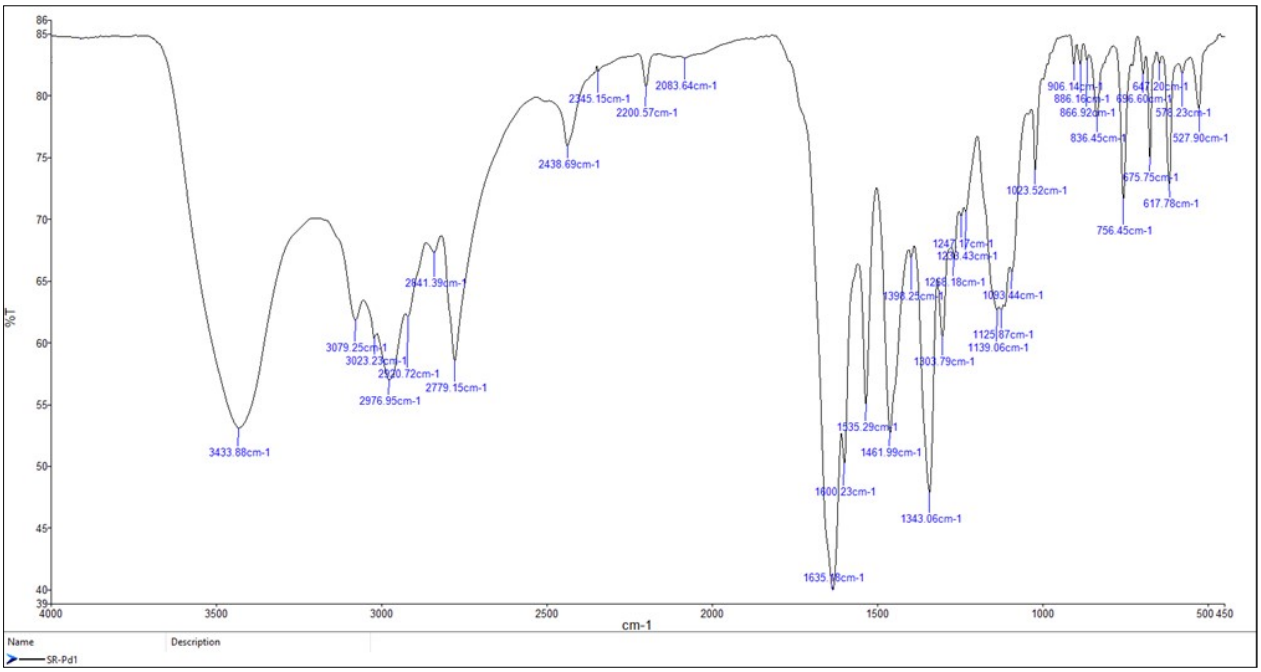

Fig. S1. IR spectrum of Pd1 complex.

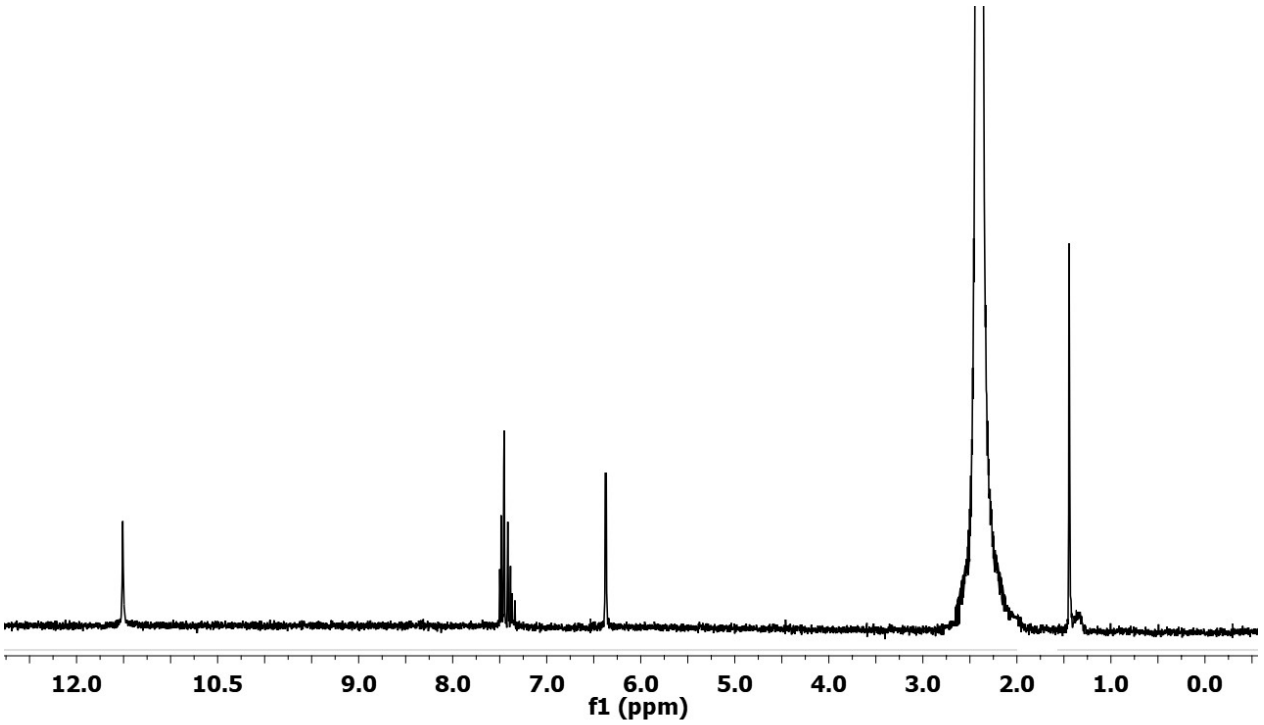

Fig S2. ^{1}H NMR spectrum of Pd1 complex.

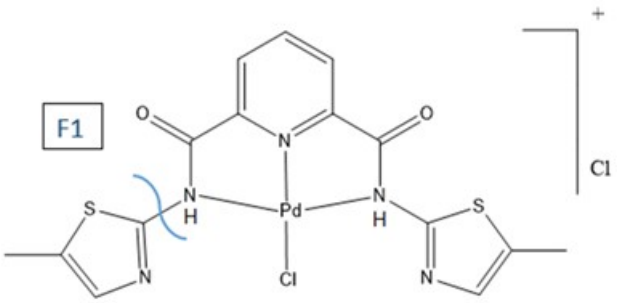

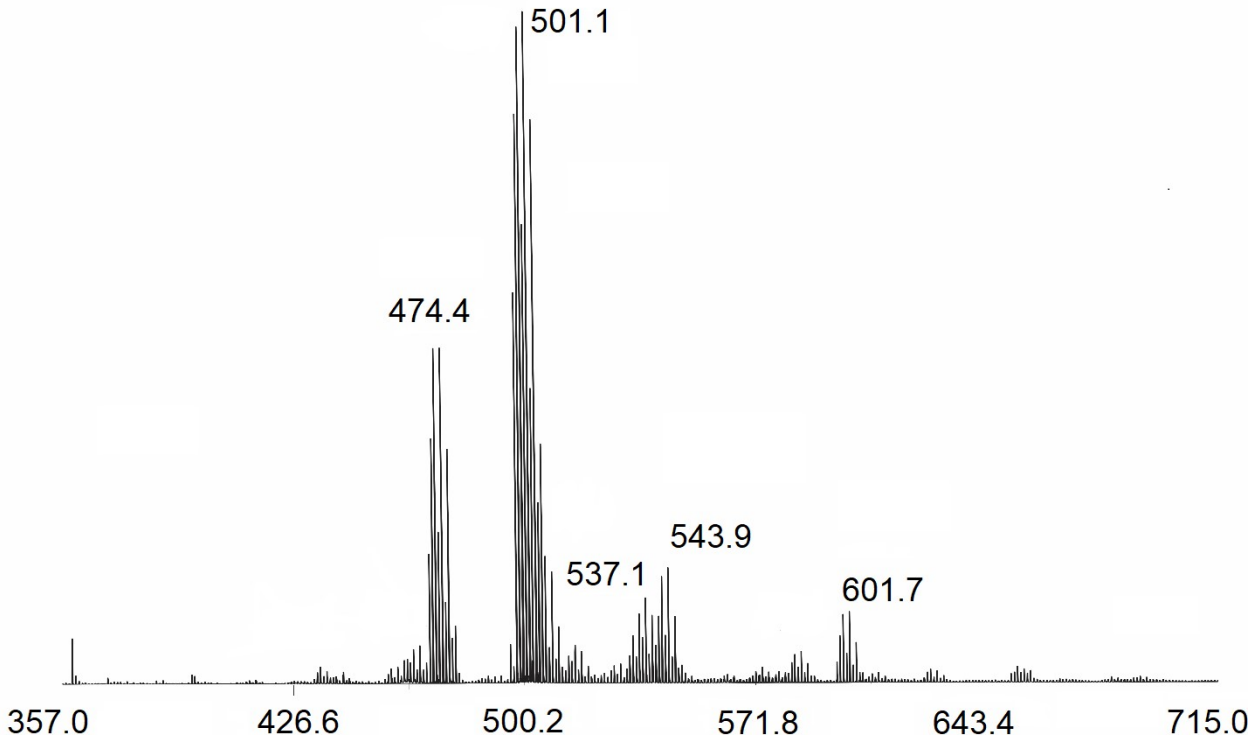

Fig S3. Positive ion mode LDI mass spectrum of Pd1 complex.

mass (*m/z*)	Signal assignment
474.4	$[Pd1^{II}\text{-}F1+2H_2O]^{\bullet+}$
501.1	$[Pd1^{II}\text{-}Cl^-]^+$
537.1	$[Pd1^{II}\text{-}Cl^-+2H_2O]^+$
543.9	$[Pd1^{II}\text{-}2F1+2DMF+K^++H_2O]^+$
601.7	$[Pd1^{II}\text{-}F1+DMF+5H_2O]^{\bullet+}$

Table S1. Assignments of *m/z* values in LDI mass spectrum of Pd1 complex detected in positive ion mode.

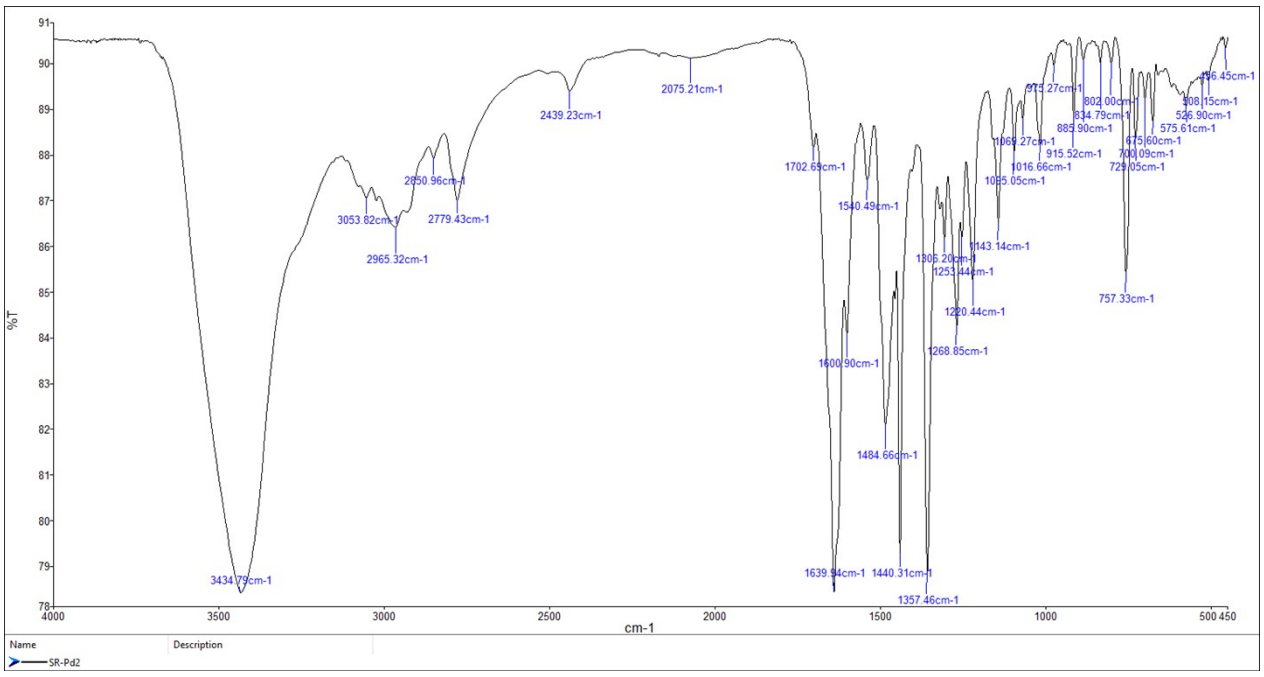

Fig. S4. IR spectrum of Pd2 complex.

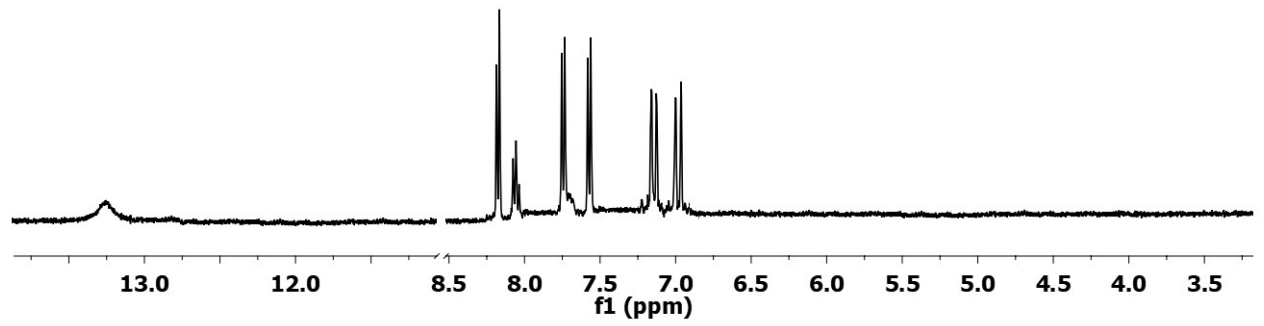

Fig S5. ^{1}H NMR spectrum of Pd2 complex.

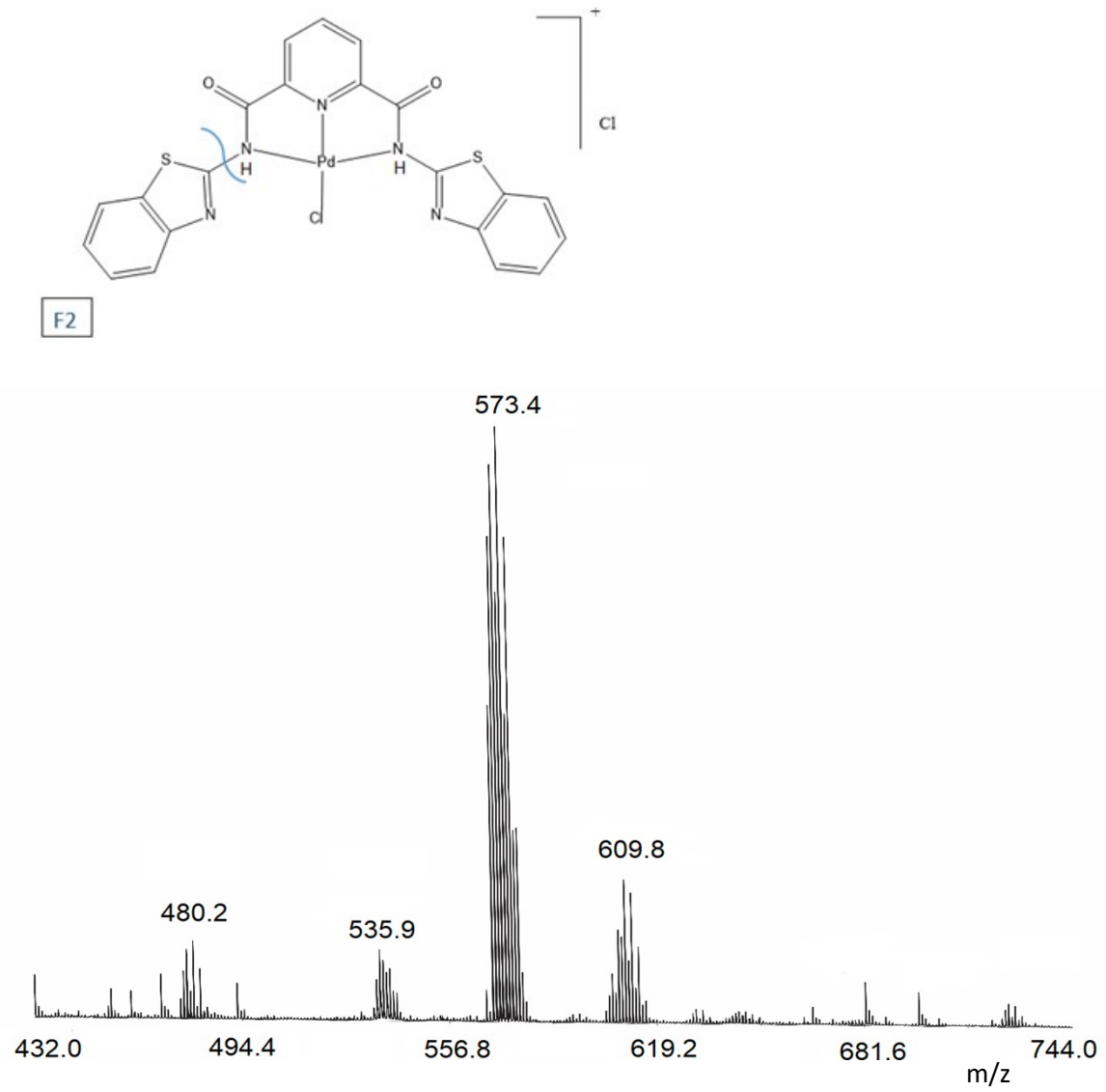

Fig S6. Positive ion mode LDI mass spectrum of Pd2 complex.

Table S2. Assignments of *m/z* values in LDI mass spectrum of Pd2 complex detected in positive ion mode.

mass (m/z)	Signal assignment
480.2	$[Pd2^{I}\text{-}F2\text{-}Cl^{-}+H_2O+Na^{+}]^{+}$
535.9	$[Pd2^{I}\text{-}2Cl^{-}\text{-}2H^{+}]^{+}$
573.4	$[Pd2^{II}\text{-}Cl^{-}]^{+}$
609.8	$[Pd2^{II}+H^{+}]^{+}$

Table S3. Observed *pseudo*-first order rate constants as a function of ligand concentration for the substitution reactions of Pd1 complex at pH = 7.2 (25 mM Hepes buffer) with addition of 50 mM NaCl at 37 ºC.

	λ [nm]	10^3 [Nu]/M	k_{obsd}/s^{-1}
L-Met	280	0.5	2.03(6)[a]
		1.0	4.32(6)
		1.5	6.70(4)
		2.0	8.52(4)
		2.5	10.08(4)
L-Cys	280	0.5	1.52(4)
		1.0	3.41(4)
		1.5	4.80(5)
		2.0	6.18(4)
		2.5	7.89(4)
5'-GMP	315	0.5	1.43(4)
		1.0	2.69(4)
		1.5	3.83(4)
		2.0	4.95(4)
		2.5	6.23(5)

[a]Number of runs.

Table S4. Observed *pseudo*-first order rate constants as a function of ligand concentration for the substitution reactions of Pd2 complex at pH = 7.2 (25 mM Hepes buffer) with addition of 50 mM NaCl at 37 ºC.

.

	λ [nm]	10^3 [Nu]/M	k_{obsd}/s^{-1}
L-Met	280	0.5	1.72(5)[a]
		1.0	3.90(4)
		1.5	6.20(4)
		2.0	7.60(5)
		2.5	9.25(5)
L-Cys	280	0.5	1.20(6)
		1.0	2.89(5)
		1.5	4.00(4)
		2.0	5.48(4)
		2.5	6.45(4)
5'-GMP	315	0.5	0.92(6)
		1.0	1.80(5)
		1.5	2.97(5)
		2.0	3.68(4)
		2.5	4.39(5)

[a]Number of runs.

Table S5. MVD-related scoring function values for Pd1 complex docked into the HSA protein binding site IIA.

complex	MolDock	Rerank	Hbond	Docking
Pd1[a]	-136.75	-79.71	-0.45	-139.56
Pd1[b]	-127.07	-24.16	-3.72	-126.99
[a]According to MolDock scoring function, the best complex pose.				
[b]Best complex pose according to Hbond scoring function.				

Table S6. MVD-related scoring function values for Pd1 complex docked into the HSA protein binding site IIIA.

complex	MolDock	Rerank	Hbond	Docking
Pd1[a,b]	-62.04	-21.33	-0.52	-49.35
[a]According to MolDock scoring function, the best complex pose.				
[b]Best complex pose according to Hbond scoring function.				

A) B)

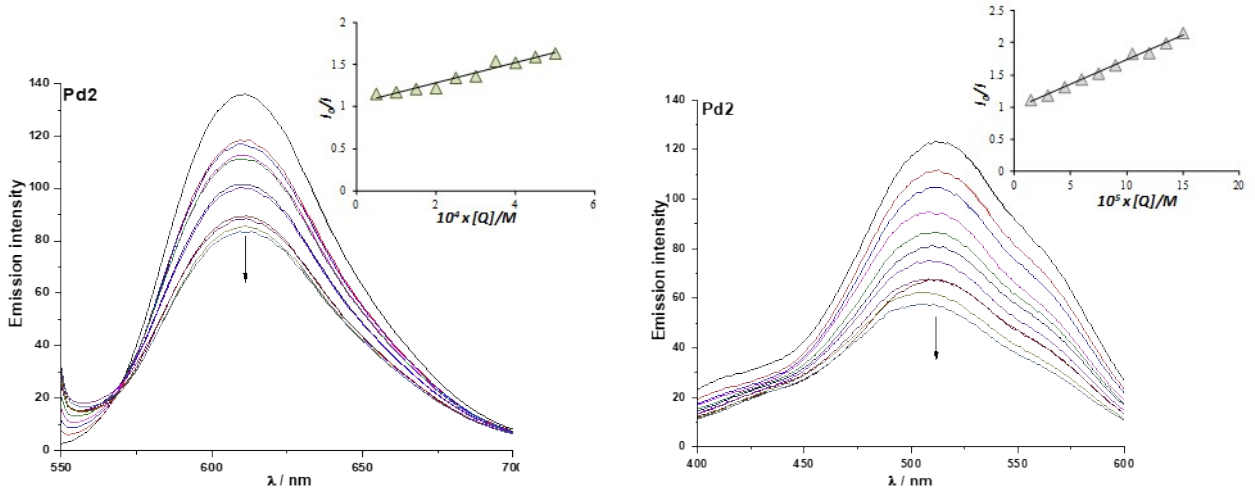

Fig. S7. A) Emission spectra of EB-DNA in the presence of complex Pd2. [EB] = 50 μM; [DNK] = 50 μM; [complex] = (50 - 500) μM; λ_{ex} = 527 nm. B) Emission spectra of HOE-CT-DNA in the presence of complex Pd2. [HOE] = 50 μM; [DNA] = 50 μM; [complex] = (15 - 150) μM; λ_{ex} = 346 nm. Arrows show the intensity changes upon increasing the concentration of complex. Insert graph: Plot of I_0/I vs. [Q].

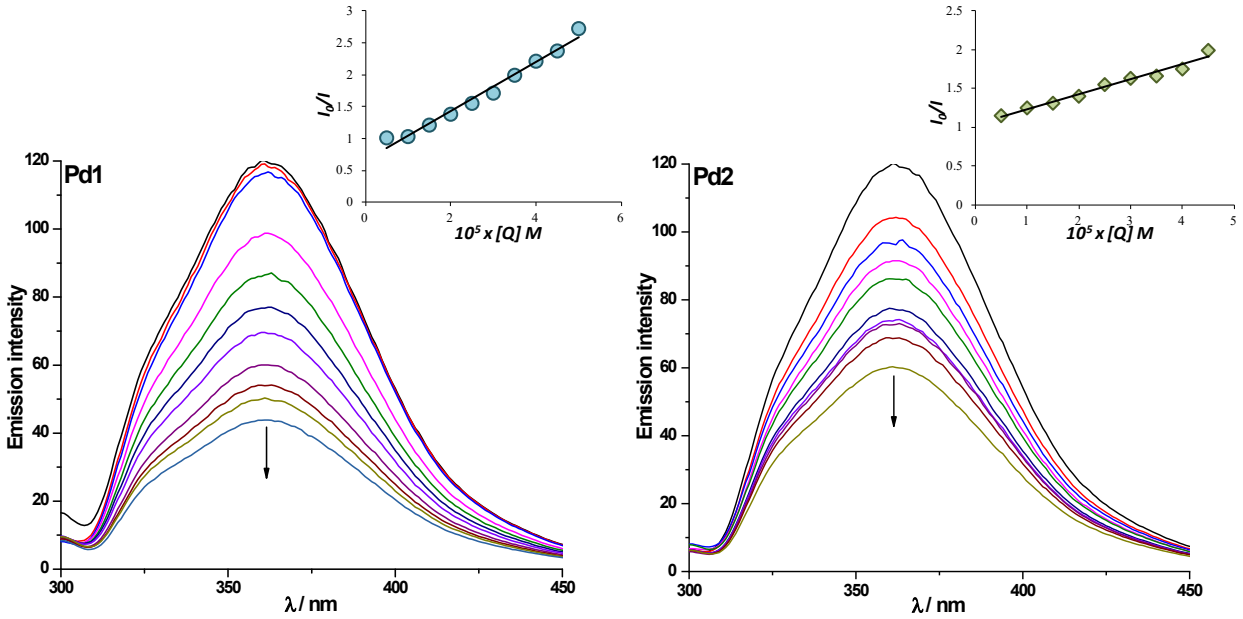

Fig. S8. Emission spectra of HSA in the presence of complexes Pd1 and Pd2. [HSA] = 50 μM, [complexes] = 5 – 50 μM; λ_{ex} = 295 nm. Arrow shows the changes in the emission intensity upon increasing the concentration of complexes. Insert graph: Stern-Volmer quenching plot of HSA for complexes Pd1 and Pd2.

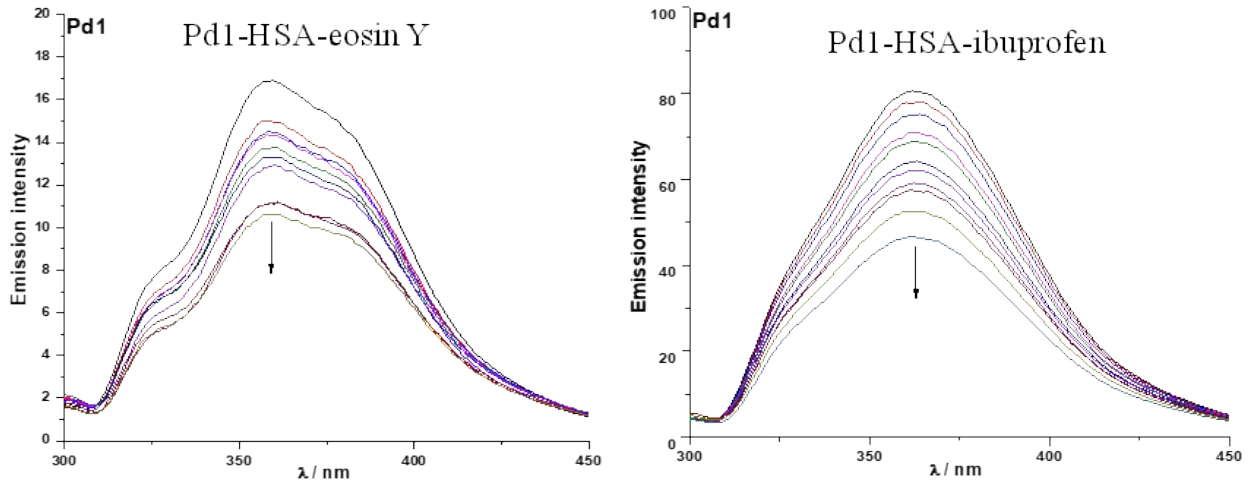

Fig. S9. Emission spectra of HSA-eosin Y and HSA-ibuprofen in the presence of complex Pd1. [HSA] = 50 μM, [eosin Y] = 50 μM, [ibuprofen] = 50 μM [complex] = 5–50 μM; λ_{ex} = 295 nm. Arrow shows the changes in the emission intensity upon increasing the concentration of complex.

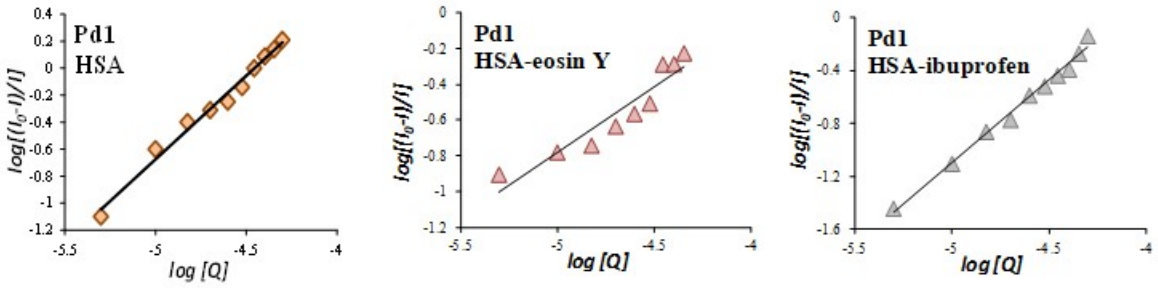

Fig. S10. Dependency of log [(I_0-I)/I] *vs*. log [Q] for the interactions of Pd1 with HSA, HSA-eosin Y or HSA-ibuprofen.

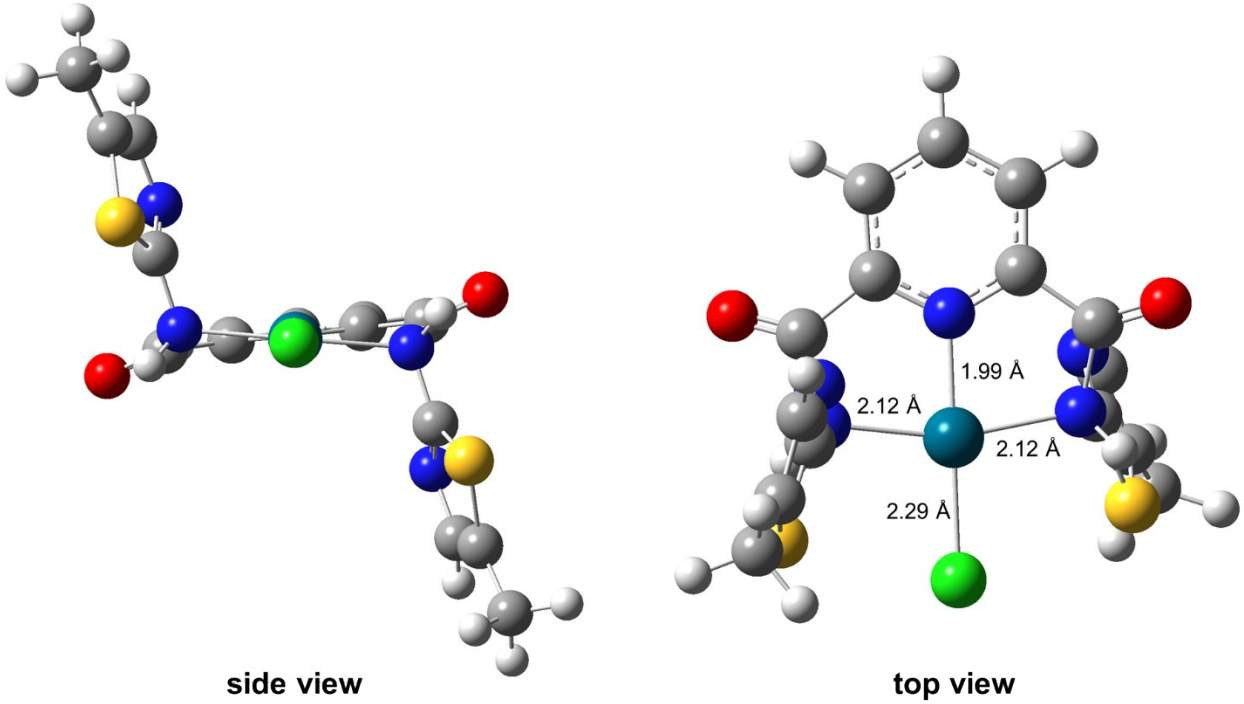

Fig. S11. Calculated (B3LYP/def2-SVP) structure of the Pd1 complex presented with the bond distances around the Pd(II) metal center.

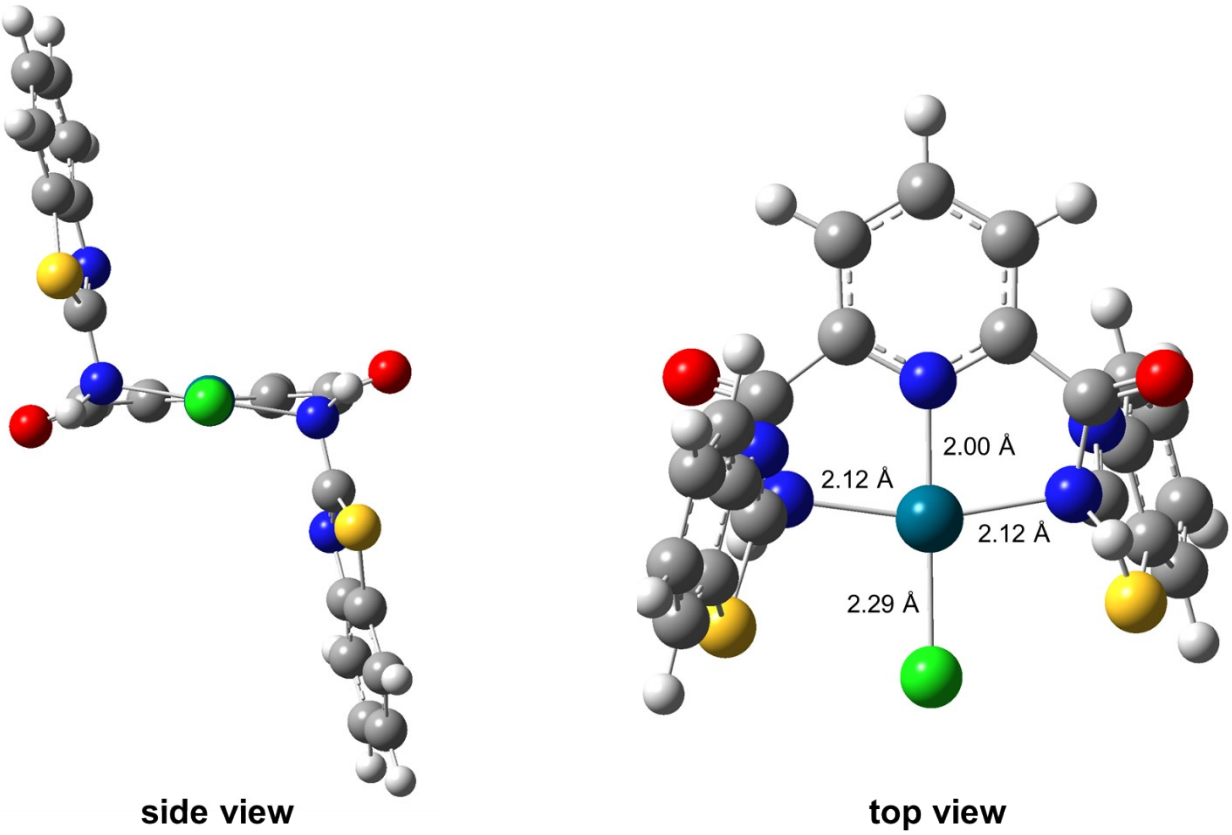

Fig. S12. Calculated (B3LYP/def2-SVP) structure of the Pd2 complex presented with the bond distances around the Pd(II) metal center.

A) B)

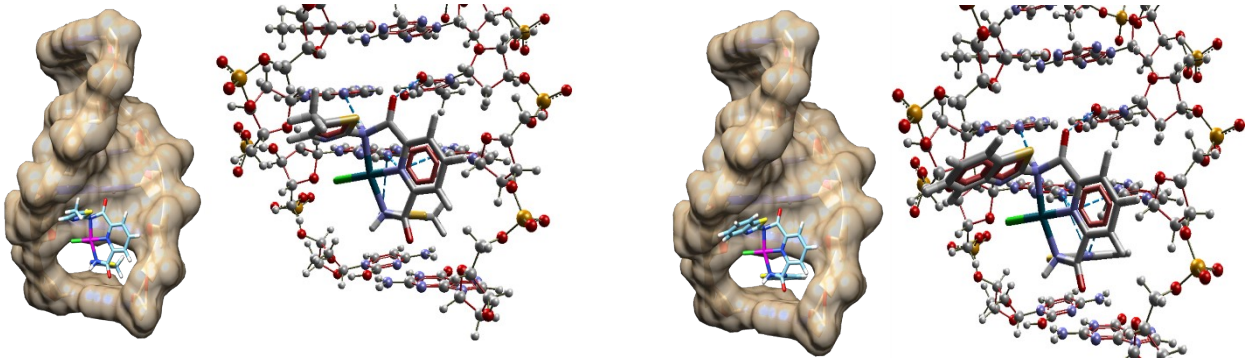

Fig. S13. Computational docking model illustrating interactions between complex A) Pd1 or B) Pd2 and DNA with the intercalation gap (1Z3F) (dotted lines display a possibility of forming hydrogen bonds).

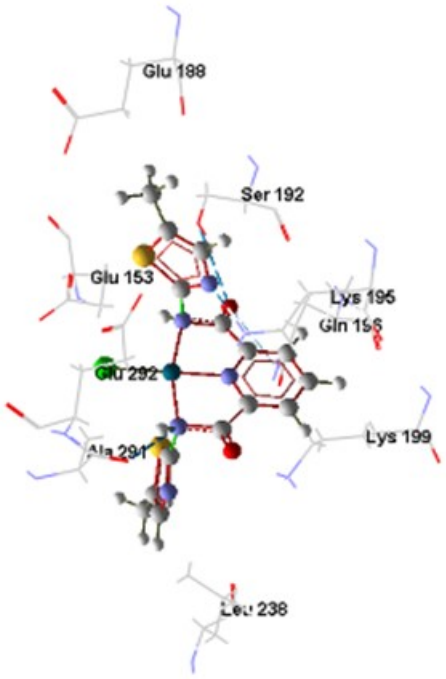

Fig. S14. Best pose with HSA docked into a subdomain IIA for complex Pd1 according to Hbond with selected amino acid residues (selected by applying an energy threshold of 0.625) represented by stick models (hydrogen bonds are shown as blue dotted lines).

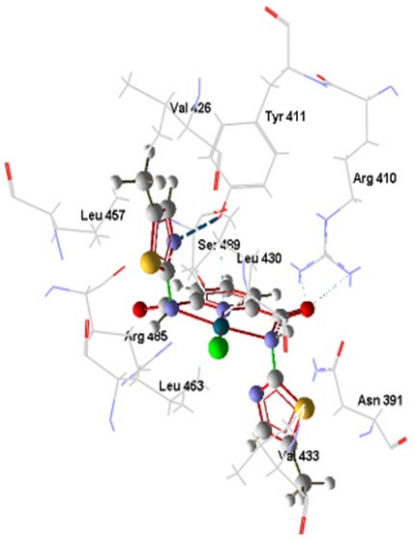

Fig. S15. Best pose with HSA docked into a subdomain IIIA for complex Pd1 according to Hbond with selected amino acid residues (selected by applying an energy threshold of 0.625) represented by stick models (hydrogen bonds are shown as blue dotted lines).

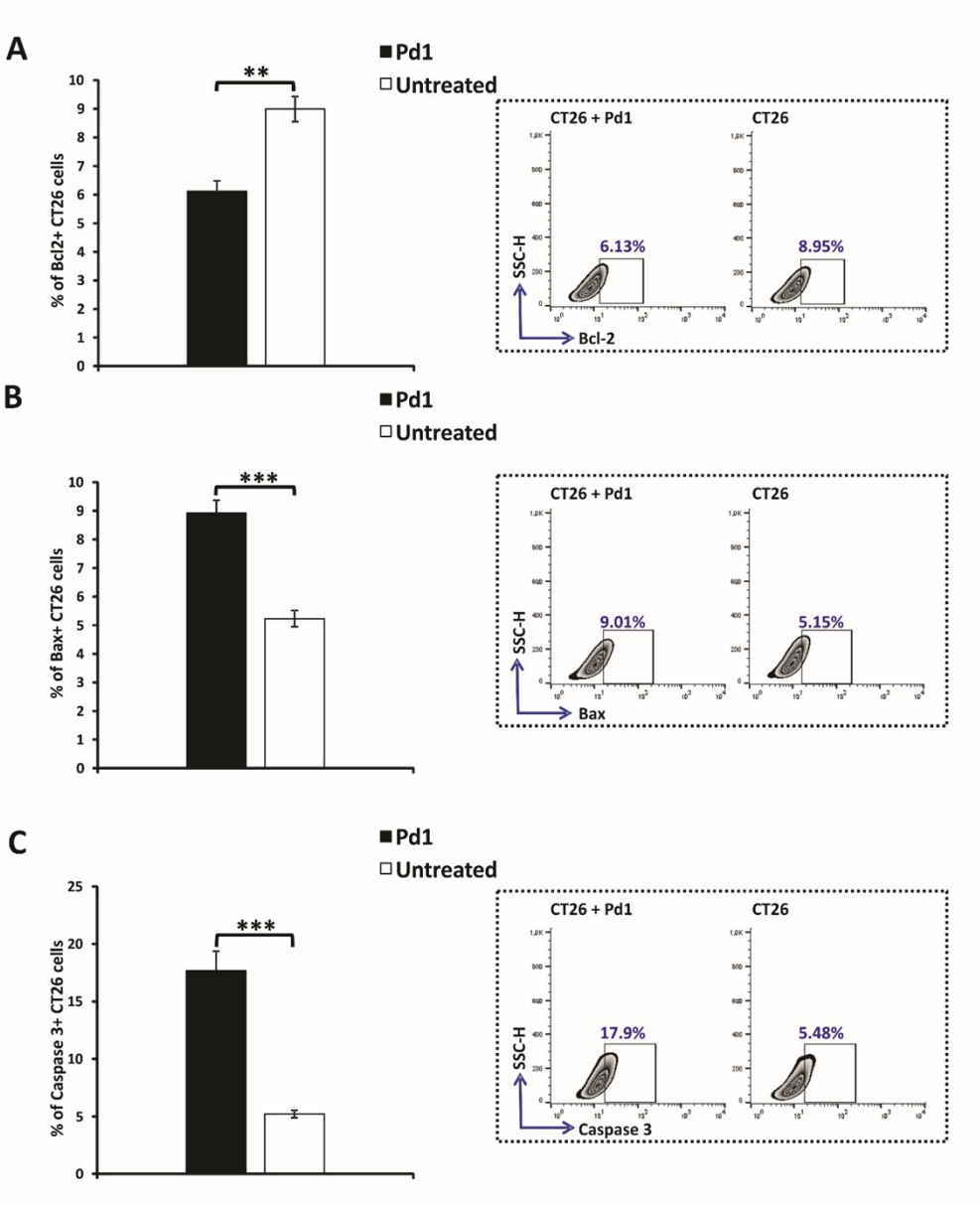

Fig. S16. The Pd1 complexes induce apoptosis of CT26 cells by controlling the expression of apoptosis-related proteins in the tumor cells. The flow cytometry evaluation of crucial apoptosis-related proteins and the enzyme caspase in tumor cells showed the expression of (A) Bcl2 and (B) Bax proteins in both untreated CT26 cells and those treated with the Pd1 complex. Panel (C) presents the expression of caspase-3 in treated versus untreated mouse CT26 colorectal carcinoma cells. The results are presented as means ± SEM from three independent experiments. Statistical significance is indicated by ** $p < 0.01$, and *** $p < 0.001$.

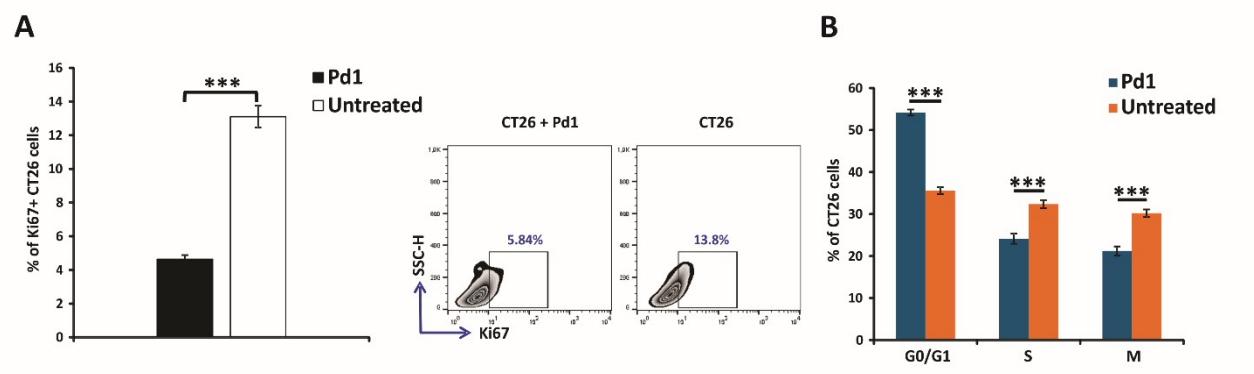

Fig. S17. Effects of Pd1 complex on Ki67 expression and cell cycle dynamics in CT26 cells. In panel A, representative FACS plots display the levels of Ki67 expression in CT26 cells after 24 hours of treatment with the compounds. Panel B highlights the impact of these compounds on the cell cycle distribution, comparing untreated and treated CT26 colorectal carcinoma cells. These effects were measured using flow cytometry and presented as the mean ± SEM based on data from three independent experiments. The statistical significance is indicated by *** $p < 0.001$, highlighting the differences in the expression of these proteins between the treated cells and the untreated control group.

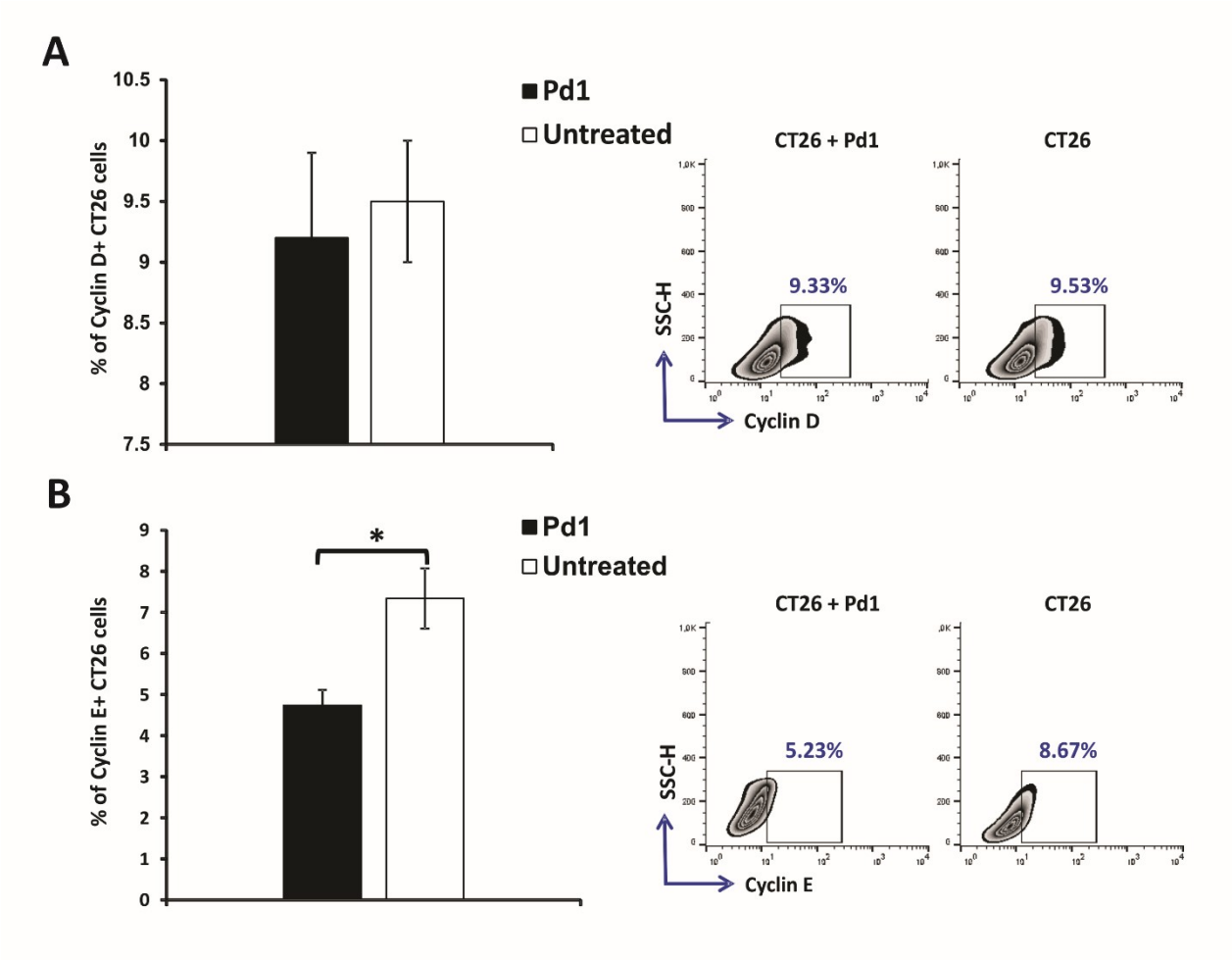

Fig. S18. Expression of cyclins in CT26 cells treated with Pd1 complex. This figure shows representative FACS plots detailing the expression of cyclins in CT26 cells after 24-hour exposure to the Pd1 complex. Panel A presents the expression of cyclin D in the cells while panel (B) shows the levels of Cyclin E. These findings, derived from flow cytometric analysis, are represented as mean ± SEM, based on data from three separate experiments. Statistical significance is indicated by *$p < 0.05$.

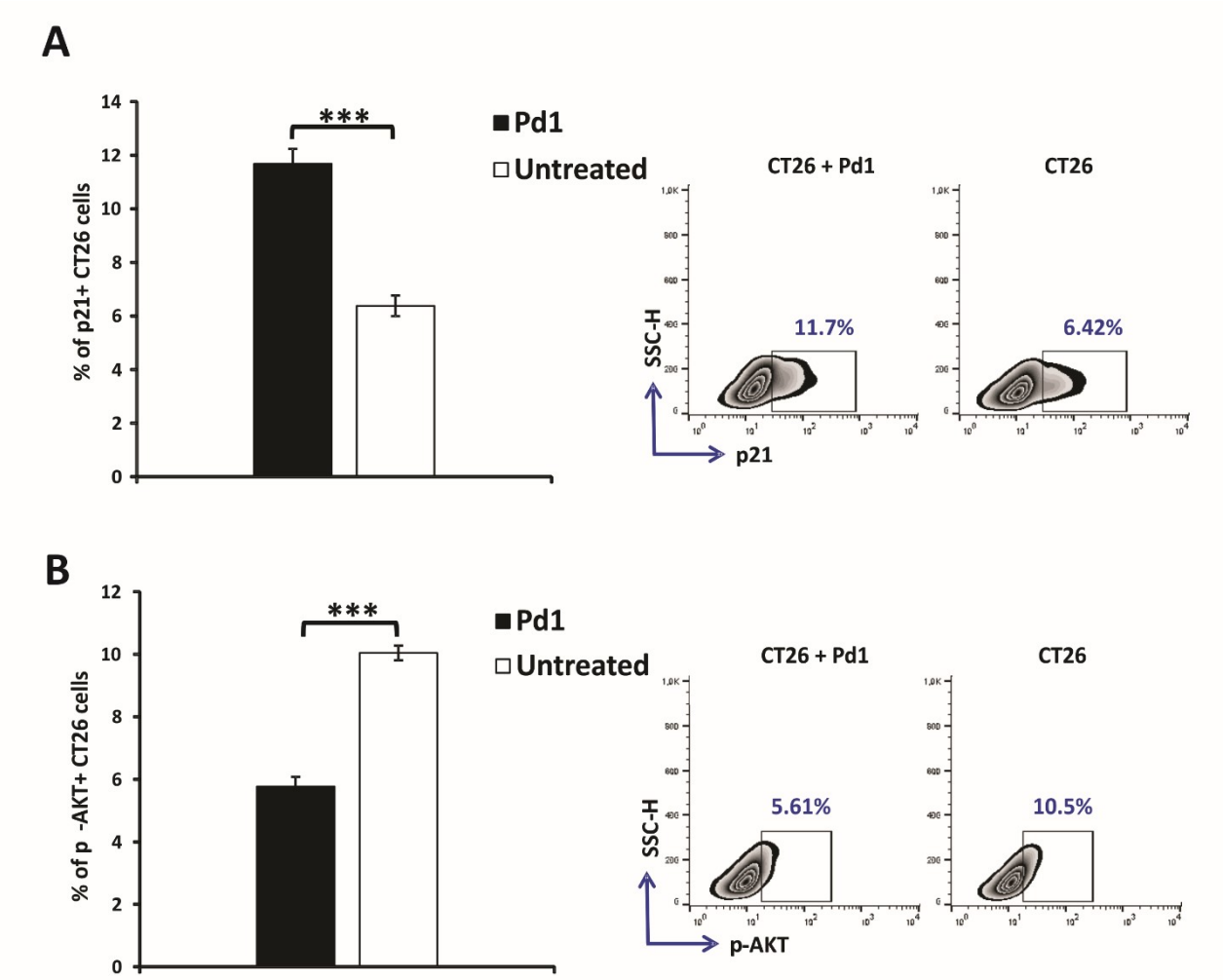

Fig. S19. The Pd1 complex controls the expression of p21 and phospho-AKT (p-AKT) in cell cycle regulation. The figure illustrates representative FACS plots that show the expression of p21 and p-AKT in CT26 cells after 24-hour exposure to the Pd1 complex. Panel A displays the expression of p21, while panel B shows the levels of p-AKT. These results, obtained from flow cytometric analysis, are presented as mean ± SEM, based on data from three separate experiments. Statistical significance is denoted by *** $p < 0.001$.